

# Selective Detection of Alkanolamine Vapors by Ion Mobility Spectrometry with Ketone Reagent Gases

T. H. Gan\*

Aeronautical and Maritime Research Laboratory, Defence Science and Technology Organization, PO Box 4331, Melbourne, Victoria 3001, Australia

G. Corino

Division of Wool Technology, Commonwealth Scientific & Industrial Research Organization, Geelong Laboratory, PO Box 21, Belmont, Victoria 3216, Australia

**The ion mobility (IMS) spectra of the alkanolamines, monoethanolamine (MEA), 3-amino-1-propanol (PRA), 4-amino-1-butanol (BUA), and 5-amino-1-pentanol (PEA) with acetone and 4-heptanone reagent gases have been measured using a hand-held spectrometer. Monomer and dimer peak patterns were observed for all the alkanolamines with acetone reagent gas. Drift times of monomer and dimer ion clusters for each alkanolamine increased linearly in order of size of alkyl group. Ammonia, Freon 22, and F76 diesel vapors, having similar or coincident mobilities, caused severe interference. Replacement of acetone with 4-heptanone reagent gas resulted in good separation by the altering drift times of product ions. The limit of detection was 0.005 ppm having a linear range of 0.005–0.7 ppm, and signal saturation occurred above 0.88 ppm. Detection was reversible, with a response time of 4 min and a slower recovery time of > 60 min, at vapor levels of 0.7 ppm and ambient nozzle and drift-region temperatures. In contrast to acetone chemistry, single-peak patterns were observed for the alkanolamines with the 4-heptanone reagent. Further, drift times unexpectedly remained stagnant with increasing alkyl-group size. From atmospheric pressure chemical ionization (APCI) tandem mass spectral identifications and collision induced studies, dynamic changes in product-ion equilibria in the IMS drift region compensated by differences in collision cross sections were suggested as the governing causes of the unusual mobility effect.**

The use of alkanolamines, including monoethanolamine (MEA), as the scrubbing agent for continuous carbon dioxide removal from submarine atmospheres<sup>1,2</sup> can lead to inhalation exposures arising from spills during maintenance operations or leakages from the scrubbing unit and/or associated plumbing. In the submarine

environment, the Maximum Permissible Concentration for continuous exposure for 90 days is 0.5 ppm.<sup>3</sup> Such low exposure levels require a method of detection which is continuous, rapid, and reversible. The presence of other pollutants affecting submarine air quality<sup>4</sup> also imposes a rigorous demand for the elimination of interferences originating from their simultaneous occurrence. This is particularly so with ammonia which is a major degradation product of MEA.<sup>2</sup>

At present, ammonia and MEA in submerged vessels are routinely determined by colorimetric-based methods<sup>2</sup> at  $\leq 1$  ppm in air. Other possible commercially available monitors employ potentiometric methods or photoacoustic spectroscopy using narrow bandwidth optical filters. However, these techniques suffer from inherent limitations such as the need to use an oven for observation of the color band or false responses due to cross interferences and limits of detection higher than 0.5 ppm. Optical sensors have also been proposed, however these devices are generally lacking in sensitivity with reported threshold limits of 24 ppm<sup>5</sup> and have poor discrimination of sensing responses from chemically related vapors.

Ion mobility spectrometry (IMS) offers very high sensitivity and is available in the form of small, portable monitors which have been deployed for the detection of chemical warfare agents<sup>6,7</sup> and used in submarines for monitoring torpedo propellant.<sup>7</sup> A detailed treatment of the subject has been provided in comprehensive reviews<sup>6,8</sup> and a recent monograph.<sup>7</sup> Essentially, the process involves ionization of vapors through a series of charge-transfer reactions between the analyte and reactant ions in the ion source region of the instrument at atmospheric pressure. These reactions are competitive, depending on relative proton affinity and analyte concentration, and provide an initial level of selectivity in detection. The product ions formed are injected into the drift tube and

\* Corresponding author: (fax) 011-61-3-96-268-409; (e-mail) tiang-hong.gan@dsto.defence.gov.au.

(1) Coverdale, A.; Cassidy, S. *Nav. Eng. J.* **1987**, 30, 528–44.

(2) Williams, D. D. Determination of Monoethanolamine and Ammonia Vapours in Submarine Atmospheres. In *The Present Status of Chemical Research in Atmosphere Purification and Control on Nuclear-Powered Submarines*; Miller, R. R., Piatt, V. R., Eds.; U. S. Naval Research Laboratory (NRL) Report 5465; April 21, 1960; pp 51–53.

(3) Royal Australian Navy Submarine Safety Manual ABR6105 – Collins Class Air Purification Manual, Department of Defence (Navy Office), Australia, November 1994.

(4) Hanhella, P. Defence Science and Technology Organisation (DSTO), Department of Defence, Australia, personal communication, April 1995.

(5) Charlesworth, J. M.; McDonald, C. A. *Sens. Actuators, B* **1992**, 8, 137–42.

(6) Eiceman, G. A. *Crit. Rev. Anal. Chem.* **1991**, 22, 17–36.

(7) Eiceman, G. A.; Karpas, Z. *Ion Mobility Spectrometry*; CRC Press: Boca Raton, FL, 1994.

(8) St. Louis, R. H.; Hill, H. H., Jr. *Crit. Rev. Anal. Chem.* **1990**, 21, 321–55.

transported through a weak electric field with characteristic drift times. The resulting ion mobilities are dependent on product ion size, shape, and charge distribution and so provide a further form of specificity to detection.

Recently, Eiceman, Limero, and co-workers explored new ionization chemistry involving the IMS of hydrazine, monomethylhydrazine, and ammonia and found that the use of 5-nonanone reagent gas resulted in good separation of production peaks of the analytes.<sup>9</sup> This significant advance provides a new capability for the highly selective detection of basic vapors. Using this development, a study of the IMS of MEA and related alkanolamines was initiated in this laboratory, since their strong proton affinities were expected to accord preferential ionization.

Although limitations of the design features of the IMS relating to adsorption on surfaces and complications from side reactions involving water chemistry were known,<sup>7,9</sup> the primary aim of this investigation was to determine whether the use of 4-heptanone reagent would impart different product-ion drift times, eliminating interference due to the simultaneous presence of vapors in the submarine atmosphere from diesel fuel (F76), Freon-22, halogenated solvents, H<sub>2</sub>S, HCl, torpedo propellant, cooking vapors, and ammonia. The study also included an understanding of the factors influencing the IMS behavior of the alkanolamines, and this required the use of atmospheric pressure chemical ionization mass spectrometry (APCI-MS) and APcI tandem mass spectrometry (APcI MS/MS) for identification of ion clusters and the determination of fragmentation cross sections as a measure of their relative stabilities.

## EXPERIMENTAL SECTION

**Ion Mobility Spectrometers.** Two standard hand-held IMS military chemical agent monitors (CAM-2) from Graseby Dynamics Ltd. (Watford, Herts, UK) were used and operated in the positive-ion mode. One CAM-2 was fitted with the standard acetone reagent gas permeation source. The other used 4-heptanone (4-hep) as the reagent gas. Briefly, the 4-heptanone diffusion source was constructed<sup>10</sup> from a 10-mm length of standard 4.8-mm internal diameter Teflon tubing with a 0.25-mm wall thickness. The tubing was filled with 250  $\mu$ L of 4-heptanone adsorbed on 500 mg of Porapak Q. A 0.25-mm hole, pierced with a syringe, gave a measured effusion rate, from four mass loss determinations, of  $2.5 \pm 0.2 \mu\text{g min}^{-1}$  or a 4-heptanone vapor level of about  $1.3 \pm 0.2$  ppm over a 24-h period. This is in agreement with the rate of loss expected from the application of Graham's Law of Effusion.<sup>11</sup>

All spectra were time-averaged using the Advanced Signal Processing (ASP) board and software (Graseby Dynamics) with an IBM-AT compatible PC operating on a repetitive 512 point drift time sweep with 64 scans per spectrum. Each spectrum was a time-averaged result over a 10-ms period. The IMS drift times of spectra displayed were referenced to the acetone reactant ion peak (RIP). The reduced mobilities,  $K_0$ , were reported using the following relationship<sup>7</sup>

$$K_0 = (b/Et) (P/760) (273/T) \dots \quad (1)$$

where  $T$  and  $P$  are the IMS cell temperature and atmospheric pressure, respectively,  $E$  is the electric field strength,  $b$  is the length of the drift tube, and  $t$  is the drift time, and for the acetone RIP,  $K_0$  at 21 °C was taken as  $1.80 \pm 0.02 \text{ cm}^2/\text{V s}$ .<sup>12,13</sup> However, because of the complexity and uncertainty of the composition of the ion clusters which determine the observed peak mobilities,<sup>9</sup> drift times are only shown for product ions of the alkanolamines with the 4-heptanone reagent.

MEA vapor at concentrations ranging from 0.005 and 0.1 ppm was produced from a permeation source using a generator (Kin Tek model 585) and delivered to the CAM-2 through a 50-cm length of 3-mm outer diameter Teflon tubing, located in a 2-cm  $\times$  10-cm-long glass sleeve to reduce the effects of air turbulence in the fume hood. Vapor from the generator was allowed to equilibrate with its surroundings at a temperature and flow rate specified by the manufacturer for 12 h, with equilibration periods of 30 min found to be sufficient for flow changes. MEA vapor levels calculated from the manufacturer's permeation rates were used as calibrations.

MEA concentrations between 0.1 and 1.55 ppm at room temperature were determined from mass changes in tenax adsorbent tubes which trapped MEA from a dry nitrogen stream using the vapor generation, dilution, and sampling apparatus described elsewhere.<sup>14</sup> The interferences, ammonia at  $\sim 0.25$  ppm and Freon 22 at  $\sim 1$  ppm, were prepared in Tedlar bags and sampled directly. F76 diesel interferent of undetermined concentration was sampled at ambient pressure. Vapor concentrations of the other alkanolamines were not determined. Standard-humidity atmospheres were generated by directing some of the flow of MEA in the dry nitrogen stream through the headspace of saturated salt solutions giving 44% RH and 92% RH. Humidity levels were checked with a humidity meter (Vaisala HM34). Oily atmospheres were similarly obtained with engine oil.

Permeation tubes of MEA were supplied by Kin Tek Inc., with high-purity MEA (99+%), 3-amino-1-propanol (PRA) (99+%), 4-amino-1-butanol (BUA) (98%), and 5-amino-1-pentanol (PEA) (97%) obtained from Aldrich Chemicals. Ammonia gas at  $530 \pm 50$  ppm and Freon 22 at  $96.9 \pm 1.9$  ppm were prepared by BOC Gases (Melbourne) who also supplied the ultrahigh-purity nitrogen gas used in the vapor generator. Tenax adsorbent (Alltech) was used without further treatment. Submarine F76 diesel fuel and engine oil samples were obtained directly.

**Atmospheric Pressure Ionization Tandem Mass Spectrometer.** A VG Quatro I (Micromass, UK) APcI triple quadrupole mass spectrometer was used for identification of clusters formed by reactions of alkanolamines with acetone and 4-heptanone vapors. In this regard, the mass spectrometer acted as a simulator for the IMS. The instrument was fitted with an atmospheric pressure ion source, specifically a plasma (corona) discharge source which operated in the positive mode with the discharge

(9) Eiceman, G. A.; Salazar, M. R.; Rodriguez, M. R.; Limero, T. F.; Beck, S. W.; Cross, J. H.; Young R.; James, J. T. *Anal. Chem.* **1993**, *65*, 1696–1702.

(10) Brokenshire, J. L. *Graseby Dynamics*, personal communication, April 1995.

(11) Atkins, P. W. *Physical Chemistry*; W. H. Freeman: San Francisco, 1984; Chapter 25.

(12) Preston, J. M.; Rajadhyax, L. *Anal. Chem.* **1988**, *60*, 31–4.

(13) Spangler, G. E.; Kim, S. H.; Campbell, D. N.; Epstein, J. Ionization of Organophosphates Using Acetone Reactant Ions For Ion Mobility Spectrometry; Chemical Research, Development & Engineering Center Report CRDEC-CR-88075, June 1988.

(14) Fortuin, J. M. H. *Anal. Chim. Acta* **1956**, *15*, 512–33.

pin held at 3200 V and 2–3  $\mu$ A. Vapors were introduced in a nitrogen plenum stream, which was dried using a drierite/sieve desiccant (Alltech), and flowed at 1 liter per minute through a probe modified for gas sampling. A constant flow of nitrogen drying gas in the ion source prevented further clustering reactions. Ions produced were accelerated in the region of intermediate pressure (0.8 Torr) by the voltage difference between the orifice plate (10 V to 120 V) and grounded skimmer, with the skimmer lens offset at 5 V higher. The ion beam was focused in a region having a pressure of  $1 \times 10^{-4}$  Torr using four lenses (L1–L4) prior to entering the first quadrupole region with an off-axis photomultiplier at the exit. The lens voltages were L1 35 V, L2 45 V, L3 305 V, L4 45 V. It should be noted that all voltages after the skimmer are negative for positive ions. Mass spectra without collision gas were acquired with source conditions varied to optimize observation of parent ions. MS/MS confirmations of identified clusters were obtained by selecting the ion of interest in the first set of quadrupoles, passed into the hexapole collision cell containing argon and fragments were analyzed in the third quadrupole. Operating conditions were collision voltage (CE) variable between 0 and 350 V, but 5 V typically was used, with the argon gas curtain maintained at a collision gas pressure corresponding to 50% transmission of the incident ion beam.

Collision induced dissociation (CID) studies for measurements of ion stabilities were conducted by subjecting the relevant clusters to argon collision gas in order to determine their cross sections for dissociation, using the same procedures outlined by Harden, Snyder, and Eiceman.<sup>15</sup> In these experiments, the applied orifice potential (cone voltage) was 15 V for larger product ions and 25 V for more stable clusters. Since the ion energy is determined by the skimmer-L1 potential difference, the starting potential was 35 eV for parent ions at atmospheric pressure. Using CE of 0 and 3 V, respectively, the collision energies in the laboratory frame of reference  $E_{\text{lab}}$  were 35 and 38 eV. According to the manufacturer, the energy spread produced by the ion source is typically about 1 V, although there may be a long tail extending for 5 V.<sup>16</sup> Hence, the translational energy distribution of parent ions may be a significant factor,<sup>15,17</sup> and therefore higher collision energies of 55–70 eV were also used. However, as intensities were reduced by 3 orders of magnitude, fragmentation cross sections were mainly determined at the lower collision energies. Owing to the multiple collision conditions encountered in the hexapole, the collision gas thickness (CGT) was varied between 20 and  $300 \times 10^{12} \text{ cm}^{-2}$ , which is significantly lower than CGT used in other studies,<sup>15,18</sup> attributed mainly to the shorter collision cell length (8 cm) and closed-box design with an effective volume of 78  $\text{cm}^3$ .<sup>16</sup>

The ketone reagent gas was placed in glass vials (Alltech) and sealed with Teflon tape, as the vapor pressures were sufficient to generate constant and significant quantities of (Ketone)·H<sup>+</sup> and (Ketone)<sub>2</sub>·H<sup>+</sup> ions for reaction with the alkanolamines. The effects of reaction conditions under which the ketone reagent gas and/or alkanolamine were in excess were also investigated. High-purity MEA and PRA samples were placed in open vials and vapors

presented directly to the dried nitrogen stream. Because of the presence of impurities in BUA and PEA, sample vials were initially covered with Teflon tape, to allow the more volatile impurities to diffuse faster through the membrane barrier. In this manner, APcI mass spectra of the impurities were obtained and complications in the alkanolamine APcI mass spectra due to impurity peaks were avoided. After about 30 min, purified alkanolamine vapors were then directly exposed to the dried gas stream. Impurity vapors in BUA and PEA were characterized by APcI-MS and APcI MS/MS having ion masses of  $m/z$  70 and  $m/z$  84, respectively, but these were not identified. Ammonia and Freon-22 were introduced into a T-junction at a flow rate of 1 L  $\text{min}^{-1}$  and, as required, water vapor (>30 ppm) present in the nitrogen carrier gas stream was used.

## RESULTS AND DISCUSSION

**Comparison of APcI-MS and IMS/MS Results. Reaction of 5-Nonanone and Monomethylhydrazine.** Exploitation of integrated APcI-MS and IMS findings is common<sup>19</sup> and was recently demonstrated by Eiceman, Limero, and co-workers<sup>9</sup> in studies involving the reactions of 5-nonanone with hydrazine (HZ), monomethylhydrazine (MMH), and ammonia. Using a Sciex TAGA 6000 API tandem mass spectrometer, and replacing the nitrogen plenum gas with bottled air conditioned with 5-nonanone vapors, these authors showed that the arrangement created the same ion clusters observed in the IMS/MS configuration. Consequently, the novel mobility effect regarding the unusual mobility spectral patterns was deduced as governed by changes in ion cluster equilibria due to analyte proton affinities and variation in reagent levels.

In this work, APcI mass spectra of MMH with 5-nonanone under conditions of excess 5-nonanone (5-non) reagent and excess MMH are shown in parts a and b, respectively, of Figure 1. Clearly, in Figure 1a, the relative intensities of the coexisting major product ions, including the protonated base  $\text{MH}^+$  ( $m/z$  47), protonated homodimer or dimer  $\text{M}_2\text{H}^+$  ( $m/z$  93), single ketone ion cluster (5-non)· $\text{MH}^+$  ( $m/z$  189), and diketone ion cluster (5-non)<sub>2</sub>· $\text{MH}^+$  ( $m/z$  331) where M is MMH, are consistent with the IMS/MS results described in ref 9. Since the observed mobility is the weighted average of individual mobilities<sup>12</sup> of ions coexisting in the ion swarm of the IMS drift tube, an appreciable abundance of the less stable ketone ion clusters having large CID cross sections<sup>9</sup> is reflected in a lower mobility, in agreement with the measured drift time of 13.3 ms for MMH,<sup>9</sup> which is less mobile than the RIP of 11 ms.

Although Eiceman, Limero et al. did not publish the IMS/MS spectrum of MMH with reduced 5-nonanone vapor concentration, the APcI mass spectrum in Figure 1b may give some insight into the effect of reagent concentration on IMS selectivity. In contrast to Figure 1a, the intensities of the larger (5-non)· $\text{MH}^+$  and (5-non)<sub>2</sub>· $\text{MH}^+$  ion clusters are decreased in the presence of excess MMH, and the protonated base  $\text{MH}^+$  and dimer  $\text{M}_2\text{H}^+$ , where M is MMH, have become predominant. As the collision cross sections of the protonated base and dimer should be smaller, their increased abundances in the ion swarm of the IMS drift tube may be associated with a shift of the MMH mobility peak to a lower drift time of 10 ms,<sup>9</sup> which is more mobile than the RIP of 11 ms.

(15) Harden, C. S.; Snyder, A. P.; Eiceman, G. A. *Org. Mass Spectrom.* **1993**, *28*, 585–92.

(16) Green, B. N.; Morris, M. *Micromass UK*, personal communication, May 1996.

(17) Bursey, M. M.; Blackburn, T. R.; Meyerhoffer, W. M.; Mattson, W. M. *Org. Mass Spectrom.* **1990**, *25*, 232–36.

(18) Dawson, P. H.; French, J. B.; Buckley, J. A.; Douglas, D. J.; Simmons, D. *Org. Mass Spectrom.* **1982**, *17*, 212–19.

(19) Bell, S. E.; Ewing, R. G.; Eiceman, G. A.; Karpas, Z. *J. Am. Soc. Mass Spectrom.* **1994**, *5*, 177–85.



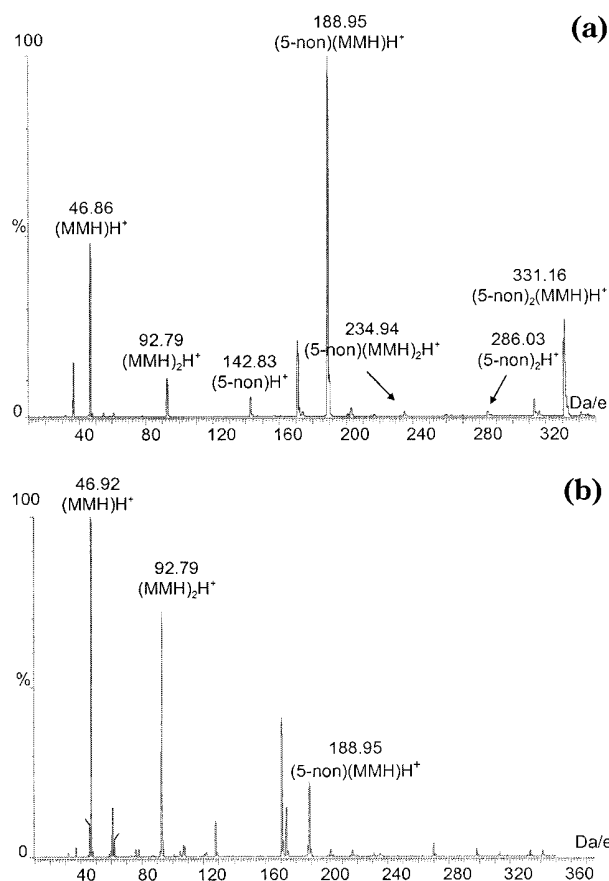


Figure 1. (a) APcI mass spectrum of product ions of 5-nonanone (5-non) and monomethylhydrazine (MMH) under conditions of a slight excess of 5-non, showing the relative abundances of  $MH^+$  ( $m/z$  47),  $(Ac)MH^+$  ( $m/z$  189),  $M_2H^+$  ( $m/z$  93), and  $(5-non)_2MH^+$  ( $m/z$  331) where  $M$  is MMH. The presence of water ( $m/z$  37),  $(5-non)H^+$  ( $m/z$  143) and  $(5-non)_2H^+$  ( $m/z$  285) reagent ions are also indicated. (b) APcI mass spectrum of product ions of 5-nonanone (5-non) and monomethylhydrazine (MMH) under conditions of excess MMH, showing the change in ion equilibria indicated by relative abundances of  $MH^+$  ( $m/z$  47),  $(5-non)MH^+$  ( $m/z$  189),  $M_2H^+$  ( $m/z$  93), and  $(5-non)_2MH^+$  ( $m/z$  331) where  $M$  is MMH.

Hence, the above APcI reaction phenomena reveal the comparability of APcI-MS and IMS results, and thus, the information may be used to provide assistance in the interpretation of mobility spectra.

#### Effect of Acetone Reagent Gas With Alkanolamine Vapors.

**IMS and APcI-MS.** Mobility spectra of MEA, PRA, BUA, and PEA with acetone reagent gas exhibit the commonly observed monomer and dimer peak pattern,<sup>9,20</sup> and their mobilities are listed in Table 1. The spectra are characterized by increasing drift times, for both monomer and dimer, which were much longer than that of the reactant ion peak (RIP) with a measured drift time of 7.3 ms at 21 °C. When the monomer and dimer drift times were plotted as a function of molecular weight of alkanolamine (Figure 2), straight lines were obtained, indicating the existence of the same ion species<sup>21</sup> for each alkanolamine monomer and dimer in the homologous series. Since the reactant ion is known to mainly comprise the protonated acetone (Ac) dimer ion,  $(Ac)_2H^+$ ,<sup>12,13</sup> the

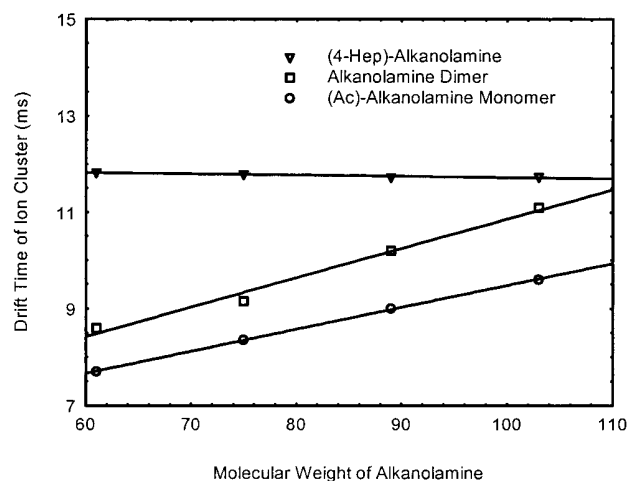


Figure 2. Variation of ion cluster drift times with molecular weight of alkanolamine showing the increasing drift times for larger acetone–alkanolamine and alkanolamine dimer clusters, but the static drift time for the 4-heptanone–alkanolamine product ions.

Table 1. Ion Mass and Reduced Mobility of Alkanolamine Clusters with Acetone Reagent Gas

cluster	ion mass (amu)	$K_0$ (cm <sup>2</sup> /V s)
acetone monomer		
(Ac)MEA·H <sup>+</sup>	120	1.68
(Ac)PRA·H <sup>+</sup>	134	1.55
(Ac)BUA·H <sup>+</sup>	148	1.44
(Ac)PEA·H <sup>+</sup>	162	1.34
dimer		
(MEA) <sub>2</sub> H <sup>+</sup>	123	1.51
(PRA) <sub>2</sub> H <sup>+</sup>	151	1.42
(BUA) <sub>2</sub> H <sup>+</sup>	179	1.26
(PEA) <sub>2</sub> H <sup>+</sup>	207	1.16

peak pattern suggests ion clusters of the type  $(Ac) \cdot MH^+$  and  $M_2H^+$  where  $M$  is the alkanolamine. The assignment of the dimer peak as most likely to belong to the  $M_2H^+$  species was based on previous observations by Karpas in his comprehensive survey of aliphatic and aromatic amines<sup>20</sup> and its intensity behavior, which decreased with time.

However, our measured reduced mobility ( $K_0$ ) at 21 °C of 1.51 cm<sup>2</sup>/V s for the MEA dimer differs from literature<sup>20</sup> values of 1.71 cm<sup>2</sup>/V s at 150 °C and 1.69 cm<sup>2</sup>/V s at 250 °C, suggesting the hydrated dimer. Although the temperature dependence of mobility for protonated aliphatic and aromatic amines of intermediate mass was rationalized as unchanged between 87 and 250 °C,<sup>7</sup> there is evidence indicating an increase in the IMS/MS observed  $K_0$  of the acetone dimer from 1.78 to 1.90 cm<sup>2</sup>/V, as the temperature was raised from 17 to 85 °C.<sup>12</sup> Thus, a small temperature variation in the  $K_0$  of the MEA dimer may occur. Further, increased charge delocalization should mitigate the influence of hydration<sup>19</sup> in the proton-bridged conformation of the MEA dimer,<sup>20</sup> and other structure-related temperature-dependent effects may become important, lending some support for our assignment at 21 °C. The second peaks of the other alkanolamines were accordingly also assigned to the dimer.

Impurity peaks in BUA and PEA were observed as doublets which decayed quickly, having measured mobilities of 1.54 and 1.66 cm<sup>2</sup>/V s for BUA and 1.48 and 1.60 cm<sup>2</sup>/V s for PEA.

(20) Karpas, Z. *Anal. Chem.* **1989**, 61, 684–89.

(21) Karpas, Z. *Struct. Chem.* **1992**, 3, 139–41.

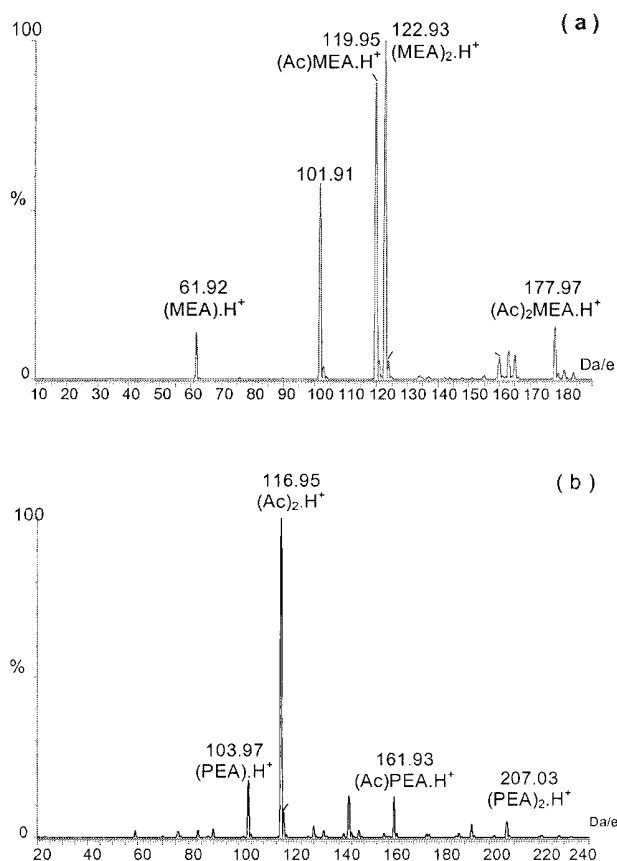


Figure 3. (a) APCl mass spectrum of product ions of acetone (Ac) and monoethanolamine (MEA) showing the relative abundances of MH<sup>+</sup> (*m/z* 62), (Ac)MH<sup>+</sup> (*m/z* 120), M<sub>2</sub>H<sup>+</sup> (*m/z* 123), and (Ac)<sub>2</sub>MH<sup>+</sup> (*m/z* 178) where M is MEA. (b) APCl mass spectrum of product ions of acetone (Ac) and pentanolamine (PEA) showing the relative abundances of MH<sup>+</sup> (*m/z* 104), (Ac)MH<sup>+</sup> (*m/z* 162), M<sub>2</sub>H<sup>+</sup> (*m/z* 207), and (Ac)<sub>2</sub>MH<sup>+</sup> (*m/z* 220) where M is PEA. Note the abundance of unreacted (Ac)<sub>2</sub>H<sup>+</sup> (*m/z* 117).

Ammonia, which appeared as a single peak with *K*<sub>0</sub> of 1.57 cm<sup>2</sup>/V s, was a trace impurity in all the alkanolamines and transited before the onset of other impurities.

APCl mass spectral data of the alkanolamines MEA and PEA with acetone reagent gas, shown in parts a and b of Figure 3, suggest that the IMS monomer peak may be associated with two coexisting product ions, predominantly the (Ac)·MH<sup>+</sup> cluster, but also the protonated base MH<sup>+</sup> at low levels. By comparison, the dimer peak may be attributed mainly to the dimer M<sub>2</sub>H<sup>+</sup> with a minor contribution from the coexisting heterodimer cluster with two ketones, (Ac)<sub>2</sub>·MH<sup>+</sup>. Essentially, there is good agreement with the IMS assignments, which implies that reactions occurring in the mass spectrometer are representative of IMS processes.

Mobility and API-MS spectra of ammonia with acetone reagent gas have been presented and discussed by Eiceman, Limero, and co-workers,<sup>9</sup> and in this study, the predominant clusters were similarly identified as the monomer (Ac)·MH<sup>+</sup> and (Ac)<sub>2</sub>MH<sup>+</sup> heterodimer, where M is ammonia. Thus, further discussion is unwarranted, other than noting that the reaction of acetone and ammonia yields more complicated product ions than reactions with alkanolamines.

**Effects of Interferent Vapors.** On exposure of the IMS to other vapors known to be present in the submarine atmosphere,

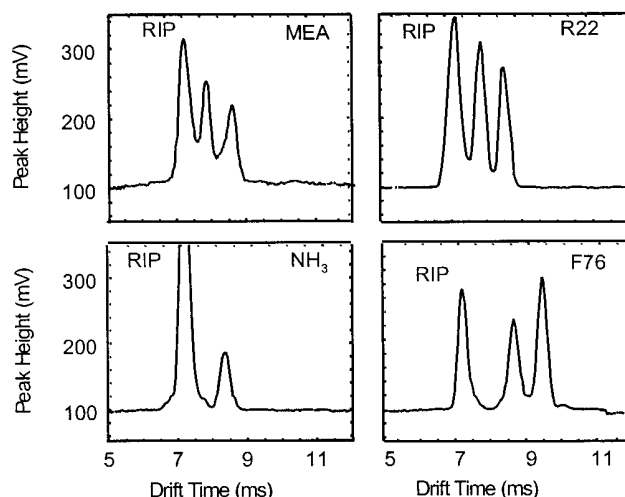


Figure 4. IMS spectra of ~0.25 ppm MEA, ~1 ppm Freon-22, ~0.25 ppm ammonia, and F76 diesel at ambient pressure with acetone reagent gas, showing the severe interference with detection of MEA.

it was found that Freon-22, diesel F76 and ammonia caused severe interference with drift times similar to that of MEA. These effects are shown in the mobility spectra in Figure 4. Ammonia is present in the atmosphere<sup>9</sup> and as a trace impurity or degradation product in commercially produced MEA.<sup>2</sup> Thus, the elimination of false alarms due to the presence of ammonia is highly desirable.

In addition, the detection of Freon-22 and diesel product ions, mainly aromatics, is surprising, since their proton affinities are lower than acetone. The drift times for product ions of Freon-22 and diesel aromatics in the presence of acetone reagent gas were longer than the RIP, suggesting cluster ions of the type (Ac)<sub>*n*</sub>·MH<sup>+</sup>, although competitive charge exchange with water reactant ions<sup>22</sup> and subsequent formation of water–Freon and water–diesel product ions was also possible. This was confirmed by monitoring the reaction products of Freon-22 and acetone in a dry and wet (>30 ppm) carrier gas stream using APCl-MS. As expected, product ion clusters were only observed for reactions of Freon-22 with water reagent, the relevant ions determined to be of the type (H<sub>2</sub>O)<sub>*n*</sub>·MH<sup>+</sup> namely trimer (*m/z* 141 and 143), pentamer (*m/z* 177 and 179), and nonamer (*m/z* 249 and 251) ion adducts. APCl mass spectral evidence for the diesel reaction products was not obtained due to the obvious difficulty posed by the complexity of the matrix. However, it is known from the literature,<sup>23</sup> that for low proton-affinity analytes, proton transfer usually occurs with water reactant ions, resulting in the formation of water-clustered product ions.

The apparent coincidence of MEA, ammonia, Freon-22, and diesel product ion drift times arising from different and competing ion chemistries indicates similarities in collisional cross sections, rather than common ion-cluster equilibria. Consequently, the use of bulkier reagents, in this case 4-heptanone, should delineate the mobilities of ketone–alkanolamine ion clusters from the more compact water–Freon or water–diesel product ions, and this is discussed below.

(22) Shoff, D. B.; Harden, C. S. Scientific Conference on Chemical and Biological Defence Research, Aberdeen Proving Ground, Maryland, November 14–17, 1995.

(23) Snyder, A. P.; Maswadeh, W. M.; Eiceman, G. A.; Wang, Y. F.; Bell, S. E. *Anal. Chim. Acta* **1995**, 316, 1–14.

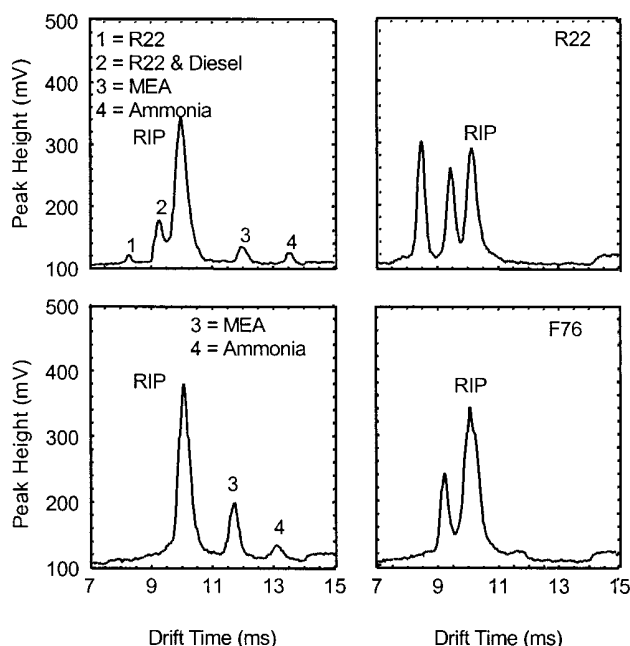


Figure 5. IMS spectra of the reactant ion peak (RIP), ~1 ppm Freon-22 (1), F76 diesel (2), ~0.25 ppm MEA (3) with ammonia trace impurity (4), at ambient pressure with 4-heptanone as the reagent gas, showing the well-resolved peaks and removal of the interference for detection of MEA.

Table 2. Effect of Humidity on Peak Height of MEA Mobility Peaks

relative humidity (%)	0.1 ppm MEA	0.25 ppm MEA
0	60 ± 5.0 <sup>a</sup> mV (8%) <sup>b</sup>	124 ± 11 <sup>a</sup> mV (9%) <sup>b</sup>
44	60 ± 5.0 <sup>a</sup> mV (8%) <sup>b</sup>	
92		126 ± 11 <sup>a</sup> mV (9%) <sup>b</sup>

<sup>a</sup> Uncertainty derived from three consecutive measurements at 1 sd. <sup>b</sup> Relative standard deviation derived from three consecutive measurements.

**Effects of 4-Heptanone Reagent Gas With Alkanolamine Vapors. IMS Spectra, Response, and Sensitivity.** Unlike the mobility spectra of the alkanolamine vapors with acetone chemistry, which show monomer and dimer peaks, only a single peak was observed with 4-heptanone reagent gas, as shown for MEA in Figure 5. It is also clear from examination of the mobility spectra of MEA at ~0.25 ppm that the use of 4-heptanone reagent gas, with an RIP at 10.1 ms, resulted in immediate and significant improvements, particularly in the separation and removal of interference by Freon-22, diesel, and ammonia. Thus, as expected, the presence of Freon-22 and diesel product ions did not interfere with the detection of MEA or ammonia with measured drift times of 11.7 and 13.2 ms, respectively. Similarly, impurity peaks in the BUA and PEA mobility spectra did not interfere with alkanolamine detection. This is indicated by PEA impurity drift times of 9.47 and 10.40 ms. Consistent with the findings of Eiceman Limero and co-workers for detection of hydrazine vapors,<sup>9</sup> the effect of increased humidity on detection of MEA at ~0.1 ppm and ~0.25 ppm was found to be negligible, as shown in Table 2. Presumably, this is attributable to the vapor-attenuating properties of the inlet membrane barrier.<sup>7,13</sup>

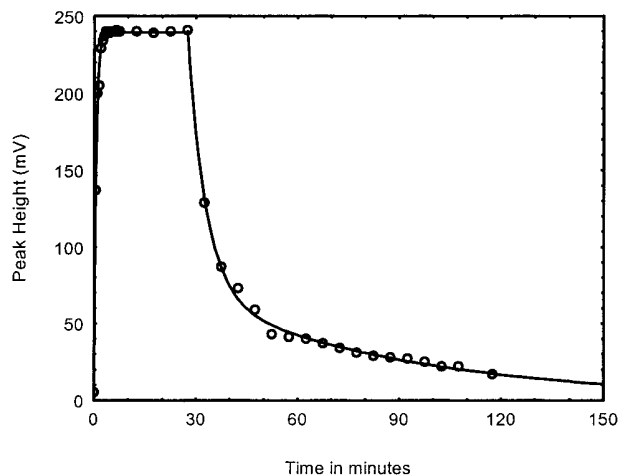


Figure 6. Variation of peak height with on-off cycle of 0.7 ppm of MEA showing the 4-min response and >60-min recovery times.

Table 3. Reproducibility of Peak Heights for MEA Product Ions in CAM-2 Using the 4-Heptanone Reagent

MEA concn (ppb)	mean peak height (mV)	sd (mv)	% relative sd	n
5	8	0.5	6	5
10	10	0.6	6	6
22	14	1	7	3
50	22	2	7	3
100	56	4	8	3
330	151			1
550	219	18	8	3
700	266			1
880	276			1
1300	273			1
1550	275			1

From Figure 6, the response time was about 4 min after start of sampling, although peaks due to formation of product ions were readily observed at 0.7 ppm after about 5 s. The recovery time was slower, at >60 min. Such long response times are most likely caused by adsorption or condensation on internal surfaces or the membrane inlet of the IMS. Similar phenomena have been observed in the use of a hand-held IMS for detection of hydrazine vapors<sup>9</sup> and may reportedly be overcome by increasing the nozzle temperature.

The limit of detection<sup>24</sup> determined for MEA was 0.005 ppm (5 ppb), from the calibration curve obtained between 0.005 and 1.55 ppm, as shown in Table 3. The reproducibility of response at 0.55 ppm was about 8% at 1 sd. The calibration curve indicates a working range between 5 and 700 ppb, with the curve plateauing above 700 ppb and saturation occurring above 880 ppb.

**Unusual Mobility Effect.** In contrast to acetone chemistry, drift times measured for the homologous series of alkanolamines with the 4-heptanone reagent did not increase with alkyl-group size. Unusual mobility effects have also been observed in the IMS of hydrazine vapors with 5-nonanone reagent by Eiceman, Limero, and co-workers<sup>9</sup> in that drift times of monomethylhydrazine (MMH), hydrazine (HZ), and ammonia increased in the order, MMH < HZ < ammonia whereas the opposite trend was intuitively expected, provided the nature of the ion clusters for each analyte were similar. These workers resorted to ion identi-

(24) Long, G. L.; Wineforder, J. D. *Anal. Chem.* **1983**, *55*, 712A–24A.

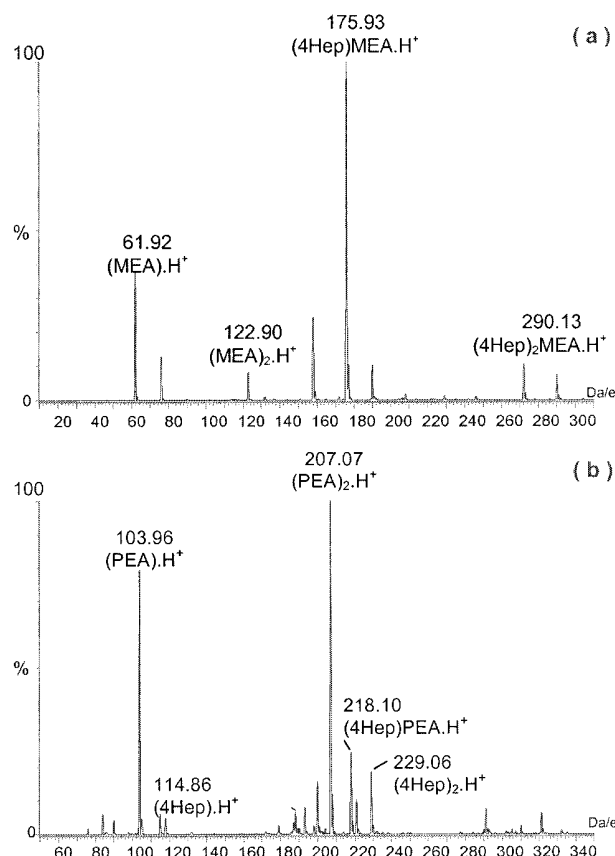


Figure 7. (a) APcI mass spectrum of product ions of 4-heptanone (4-hep) and monoethanolamine (MEA) showing the relative abundances of MH<sup>+</sup> (*m/z* 62), (4-hep)MH<sup>+</sup> (*m/z* 176), M<sub>2</sub>H<sup>+</sup> (*m/z* 123), and (4-hep)<sub>2</sub>MH<sup>+</sup> (*m/z* 290) where M is MEA. (b) APcI mass spectrum of product ions of 4-heptanone (4-hep) and pentanolamine (PEA) showing the relative abundances of MH<sup>+</sup> (*m/z* 104), (4-hep)·MH<sup>+</sup> (*m/z* 218), M<sub>2</sub>H<sup>+</sup> (*m/z* 207), and (4-hep)<sub>2</sub>·MH<sup>+</sup> (*m/z* 332) where M is PEA. Note the abundances of unreacted (4-hep)·H<sup>+</sup> (*m/z* 115) and (4-hep)<sub>2</sub>·H<sup>+</sup> (*m/z* 229).

fications using IMS/MS and CID studies with API tandem mass spectrometry and found that the reversed order of ion mobilities resulted from the differing nature and stabilities of ion equilibria coexisting in the ion swarms of the analytes passing through the drift tube region. In this study, the cause of the unchanging mobilities of the alkanolamines was elucidated using APcI-MS and APcI MS/MS for ion identifications and determinations of ion stabilities from cross sections for dissociation.

**APcI-MS and APcI-MS/MS.** As was the case of the major ions identified for 5-nonanone,<sup>9</sup> the reactant ions of 4-heptanone (4-hep) was confirmed from APcI MS/MS to comprise the (4-hep)H<sup>+</sup> and (4-hep)<sub>2</sub>H<sup>+</sup> ions having *m/z* of 115 and 229, respectively. Product ions for the alkanolamines and ammonia impurity generally included not only the protonated base MH<sup>+</sup>, monomer ion (4-hep)MH<sup>+</sup> and diketone heterodimer (4-hep)<sub>2</sub>MH<sup>+</sup>, but also the alkanolamine dimer of the type M<sub>2</sub>H<sup>+</sup>. Each product ion was characterized by APcIMS and APcI MS/MS and their coexistence is shown in the mass spectra in Figure 7. Relative abundances are also indicated, and for MEA, increased in the order

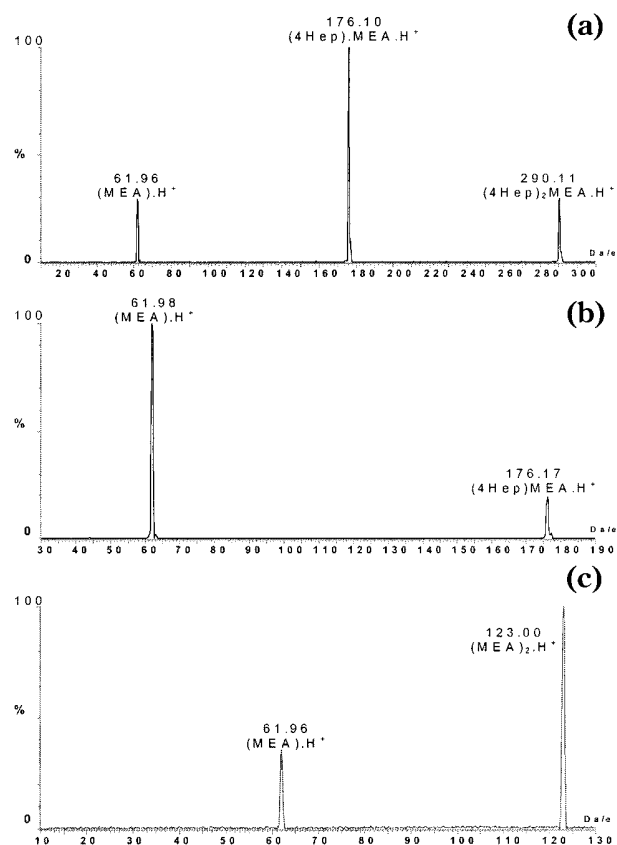
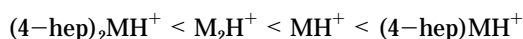
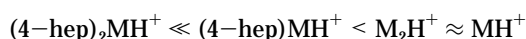


Figure 8. (a) APcI tandem mass spectrum (MS/MS) of (4-hep)<sub>2</sub>MH<sup>+</sup> (*m/z* 290) where M is MEA showing the CID loss of one and two 4-heptanones and the residual MH<sup>+</sup> (*m/z* 62). (b) APcI tandem mass spectrum (MS/MS) of (4-hep) MH<sup>+</sup> showing the CID loss of one heptanone and the residual MH<sup>+</sup> (*m/z* 62). (c) APcI tandem mass spectrum (MS/MS) of M<sub>2</sub>H<sup>+</sup> (*m/z* 123) where M is MEA showing the CID loss of M and the residual MH<sup>+</sup> (*m/z* 62).

However, with increasing size of the alkyl group of the alkanolamine, the following trend in relative abundances emerged



with the (4-hep)<sub>2</sub>MH<sup>+</sup> heterodimer barely observable for BUA and PEA, indicated by the low peak intensity of *m/z* 332 in Figure 7. From APcI MS/MS analyses shown in Figure 8 for MEA, logical neutral losses of (4-hep) or M confirmed assignments of the heterodimer, monomer, and M<sub>2</sub>H<sup>+</sup> alkanolamine dimer ions, respectively.

These unexpected changing trends may be interpreted in terms of stabilities of the ion clusters from CID experiments, even if only in qualitative terms. In their CID study of hydrazines including ammonia, with 5-nonanone, Eiceman, Limero, and co-workers demonstrated that the slopes given by the logarithm of parent ion intensity as a ratio of total ion intensity versus collision gas thickness provided quantitative information regarding relative stability of ion clusters, with large slopes indicating unstable ions.<sup>9</sup> From relative measurements of fragmentation cross sections in 4-heptanone-alkanolamine clusters,<sup>25</sup> shown in Figure 9 and listed in Table 4, stabilities of (4-hep)MH<sup>+</sup> and (4-hep)<sub>2</sub>MH<sup>+</sup> ions



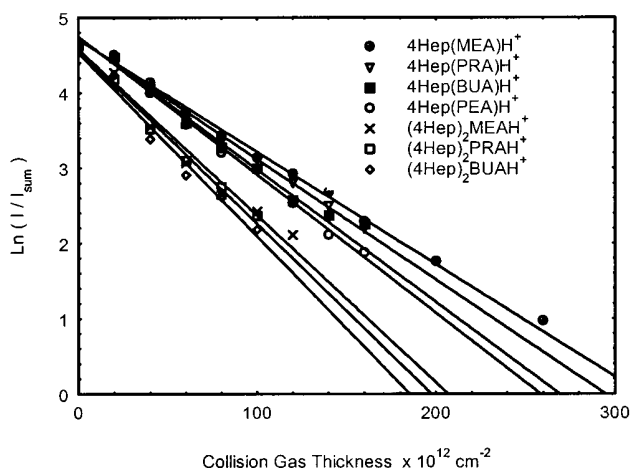


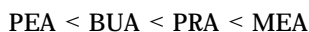
Figure 9. Relative CID cross sections of 4-heptanone-alkanolamine clusters given by slopes of the logarithm of the fraction of total cluster ion intensity versus collision gas thickness.

Table 4. Ion Mass, Reduced Mass, and Relative Stability of Ammonia and Alkanolamine Ion Clusters with 4-Heptanone Reagent Gas

cluster	ion mass (amu)	reduced mass ( $10^{-12}$ )	slope <sup>a</sup> ( $\text{\AA}^2$ )	proton affinity <sup>b</sup> (kcal/mol)
4-heptanone monomer				
(4-hep)·NH <sub>4</sub> <sup>+</sup>	132	5.30	28	204.0
(4-hep)MEA·H <sup>+</sup>	176	4.92	150	221.3
(4-hep)PRA·H <sup>+</sup>	190	4.89	159	228.6
(4-hep)BUA·H <sup>+</sup>	204	4.87	173	233.8
(4-hep)PEA·H <sup>+</sup>	218	4.85	183	
heterodimer				
(4-hep) <sub>2</sub> NH <sub>4</sub> <sup>+</sup>	246	4.82	167	204.0
(4-hep) <sub>2</sub> MEA·H <sup>+</sup>	290	4.78	221	221.3
(4-hep) <sub>2</sub> PRA·H <sup>+</sup>	304	4.77	231	228.6
(4-hep) <sub>2</sub> BUA·H <sup>+</sup>	318	4.76	245	233.8

<sup>a</sup> Slope from plot of  $\ln(I/I_{\text{sum}})$  versus collision gas thickness which gives a relative ordering of product-ion stability measured by the CID cross section. <sup>b</sup> Values from ref 28.

within the alkanolamine series were found to increase in the order



with (4-hep)<sub>2</sub>MH<sup>+</sup> ions considerably less stable than (4-hep)-MH<sup>+</sup>. Observations for ammonia were identical, as expected from the study with 5-nonanone.<sup>9</sup> Further, slopes increase with increasing alkyl-group size, indicating the increasing fragility of hydrogen bonding of the clusters. Relative stability of dimer ions of the type M<sub>2</sub>H<sup>+</sup> from a separate reaction pathway also increased in a similar trend. Although slopes of monomer and dimer were similar, ion abundances suggest that as proton affinity of analyte M increases, (4-hep)MH<sup>+</sup> ions become less stable than the M<sub>2</sub>H<sup>+</sup> dimers.

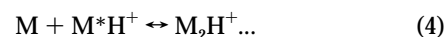
Following the inference by Eiceman, Limero, and co-workers,<sup>9</sup> the determining cause may be the proton affinities of the alkanolamines influencing ion structures. According to the findings of Hiraoka,<sup>26,27</sup> as proton affinity increased in going from MEA to PEA,<sup>28</sup> the bond energies of protonated dimers decreased and so

ion stability of (4-hep)<sub>2</sub>MH<sup>+</sup> decreases in the observed order. Moreover, the additional stability of the protonated base MH<sup>+</sup>, imparted by proton-induced cyclization,<sup>21</sup> favored M<sub>2</sub>H<sup>+</sup> dimer formation over the monomeric (4-hep)MH<sup>+</sup> species, indicated by changes in relative abundances in Figures 3 and 7. Since these spectra were acquired under conditions of reduced and excess concentrations of 4-heptanone reagent gas, observed increases in M<sub>2</sub>H<sup>+</sup> dimer ion cluster abundances, especially in the presence of the latter, suggest dynamic changes in reaction equilibria which are proton-affinity-dependent.

**Relationship Between Ion Stability, Composition, and Drift Times.** Relying on the findings of Preston and Rajadhyax,<sup>12</sup> Eiceman, Limero, and co-workers<sup>9</sup> showed, in their recent study on the IMS of hydrazine vapors, that an observed hydrazine peak mobility was the weighted average of mobilities of individual product ions, coexisting as separate equilibrium components, in an ion swarm within the drift region. Likewise, measured drift times of the alkanolamines, including ammonia, may generally be associated with four distinct and competitive ion equilibria resulting from reactions with the reactant ion monomer (4-hep)-H<sup>+</sup>, as described by the following kinetic scheme<sup>9,12</sup>



formation of protonated dimer



formation of the cluster ion with a single ketone



formation of the cluster ion with two ketones



Additional equilibria could be written for the reactant dimer ion (C<sub>7</sub>H<sub>14</sub>O)<sub>2</sub>·H<sup>+</sup> to give a protonated base and a cluster ion with a single ketone.<sup>9</sup> Structural and mechanistic details of reaction intermediates and products were not determined, although it is known from IMS studies that the protonated bases of the alkanolamines undergo intramolecular proton bridging leading to more compact ring structures.<sup>20,21</sup>

Recent findings by Eiceman, Limero and co-workers<sup>9</sup> and Eiceman, Harden, and co-workers<sup>29</sup> indicate, depending on the state of equilibrium, relative ion abundances and, hence, drift times and analytical selectivity are influenced by temperature and concentration of reagent gas. Variable temperature studies were not attempted as the commercial IMS unit used operated at a fixed temperature. To gain a qualitative understanding of the relation-

(25) Gan, T. H.; Corino, G. Presented in part at the Australian and New Zealand Society for Mass Spectrometry, 16th Conference, Hobart, Tasmania, February 2–6, 1997.

(26) Hiraoka, K.; Takimoto, H.; Yamabe, S. *J. Phys. Chem.* **1986**, *90*, 5910–14.

(27) Hiraoka, K. *Can. J. Chem.* **1987**, *65*, 1258–61.

(28) Lias, S. G.; Liebman, J. F.; Levin, R. D. *J. Phys. Chem. Ref. Data* **1984**, *13*, 695–808.

(29) Eiceman, G. A.; Wang, Y. F.; Garcia-Gonzalez, L.; Harden C. S.; Shoff D. B. *Anal. Chim. Acta* **1995**, *306*, 21–33.



ship between reagent gas concentrations and selectivity, vapor levels of 4-heptanone were varied, initially using a permeation tube which delivered about 43 ppb of reagent gas to the source and drift regions. Under these conditions, the MEA product ion was an unresolved multiplet with higher mobility than the RIP,<sup>10</sup> indicating very little selectivity. At higher vapor levels of about 0.3 ppm obtained using the diffusion source, ammonia product ions giving a small peak at 11.3 ms and a larger peak at 12.2 ms were observed. For MEA, a minor peak, which was more mobile than the RIP, appeared at 9.2 ms with the major product ion at 11.4 ms. Although there is better separation of ammonia and MEA peaks, the occurrence of interference by the minor peaks indicates a need for greater selectivity. At the operating concentration of about 1.3 ppm, mobility spectra featuring full discrimination, shown in Figure 4, were obtained. Thus, vapor levels of reagent gas, in addition to proton affinity of analyte, affect the specificity of detection.<sup>9,28</sup>

These observations for MEA suggest that lower 4-heptanone vapor levels ( $\leq 0.3$  ppm) affect the state of equilibrium such that relatively greater abundances of  $MH^+$  and  $M_2H^+$  dimer product ions coexisting in the ion swarm result in observed lower drift times. Correspondingly, with increasing 4-heptanone (4-hep) concentrations, relatively increased abundances of coexisting (4-hep)· $MH^+$  monomer and (4-hep)<sub>2</sub>· $MH^+$  heterodimer clusters lead to higher drift times. The minor peaks were not mass-identified, but may arise from formation of water adducts.

From the foregoing, it can therefore be argued that, as proton affinity increases with size of alkyl group, there is a dynamic change in product-ion equilibria favoring formation of the more stable protonated base  $MH^+$  and alkanolamine dimer  $M_2H^+$  over the (4-hep)· $MH^+$  monomer and (4-hep)<sub>2</sub>· $MH^+$  heterodimer clusters. This should be accompanied by a downward trend to lower drift times relative to MEA monomer, consistent with the equilibria written in eqs 3–6. However, with the increasing ring size of the proton-bridged dimers, their larger collision cross sections should cause a shift to progressively longer drift times. Consequently, within the homologous series of alkanolamines, these opposing factors lead to a compensating effect in mobility trends and, hence, result in measured drift times which appear unaltered.

## CONCLUSIONS

Detection of MEA and related alkanolamines in air, using IMS with acetone reagent gas is reasonably selective, characterized by peaks due to monomer (Ac) $MH^+$  and dimer  $M_2H^+$  product ions with linearly increasing drift times for the larger alkanolamines. However, for applications in submarines, the simultaneous presence of ammonia, Freon-22, and F76 diesel vapors interfered through product ions having similar or coincident drift times as those of MEA. This finding was surprising, as such dissimilar analytes were expected to give rise to ion drift times which differed significantly. Thus, although the ionization of Freon-22 and F76 diesel vapors occurred through charge-transfer reactions involving hydrated proton reactant ions, and are therefore in contrast with the product ions preferentially formed from charge exchange and clustering of ammonia and MEA with acetone reactant ions, this interference necessitated studies using alternate reagent chemistry.

Improved analytical specificity, by altering drift times of product ions and thus gaining better separation of ketone-clustered and

water-clustered peaks, was achieved with 4-heptanone (4-hep) reagent gas. In contrast to acetone chemistry, mobility spectra of alkanolamines with the 4-heptanone reagent did not exhibit monomer and dimer peak patterns. Instead, only a single peak could be assigned to detection of the alkanolamines. Further, measured drift times unexpectedly remained static with increasing size of alkyl group. Using APcI MS/MS, the relevant alkanolamine product ions with 4-heptanone (4-hep) reagent gas identified were protonated base  $MH^+$ , alkanolamine dimer  $M_2H^+$ , monomer (4-hep)· $MH^+$  and heterodimer (4-hep)<sub>2</sub>· $MH^+$ . Relative abundances of these product ions coexisting as an ion swarm in the IMS drift region, and thereby influencing the degree of analytical selectivity, were found to be highly dependent on reagent vapor levels. Lower reagent concentrations were characterized by lower analyte drift times, with mobility spectra showing complex and poorly resolved peak patterns for both analyte and ammonia interferent. By comparison, with increased ketone dopant levels, mobility spectra displaying well-separated, distinctive analyte and interferent peaks appearing at longer drift times were observed.

Abundances of the heterodimer and monomer ion clusters also quickly diminished with increasing size of the alkanolamine alkyl group, whereas abundances of the alkanolamine dimer and protonated base progressively increased. These observations were consistent with determinations of collision-induced dissociation (CID) cross sections, which suggested the following order of stabilities



As the relative stabilities of individual product ions, governed by increasing proton affinity with size of alkanolamine, affected their relative abundances in the ion swarm, then, observed drift times should be characterized by the weighted average of individual product ion drift times.<sup>9,12</sup> Consequently, the unusual IMS response in going from MEA to PEA was deduced to arise from dynamic changes in ion equilibria resulting in the formation of more stable but lower ion mass  $M_2H^+$  and  $MH^+$  compared with (4-hep)<sub>2</sub>· $MH^+$  and (4-hep)· $MH^+$  clusters. This should cause a shift to lower drift times relative to MEA. However, as the collision cross sections of the dimer  $M_2H^+$  and the  $MH^+$  protonated base increased with alkyl group, there should be a corresponding increase in observed drift times. Hence these compensating factors resulted in unchanging measured drift times for the alkanolamines. These findings, along with others,<sup>7,9</sup> suggest that IMS is likely to be useful in future studies involving the selective detection of airborne contaminants.

## ACKNOWLEDGMENT

Assistance provided by Dr. J. L. Brokenshire of Graseby Dynamics (UK) is gratefully acknowledged. We also wish to express our deepest thanks to Dr. B. N. Green and Dr. M. Morris of Micromass (UK) for their technical support and our sincere thanks to Dr. S. D. Tanner of PE-Sciex (Canada) for enlightening discussions regarding the characteristics of free-jet expansions and molecular-beam skimming in the API source. We acknowledge the help of Mr. V. Tantaró of DSTO-AMRL in the use of the vapor-calibration apparatus.

Received for review May 25, 1999. Accepted November 5, 1999.

AC990549K